Contents lists available at ScienceDirect

Electrochemistry Communications

Full Communication

Indirect electrochemical method for high accuracy quantification of protein adsorption on gold surfaces

István Bakos [a,*], Ádám Vass [a], Eric S. Muckley [b], Ilia N. Ivanov [b], Zsófia Keresztes [a]

[a] *Institute of Materials and Environmental Chemistry, Research Centre for Natural Sciences, H-1519 Budapest, P.O. Box 286, Hungary*
[b] *Center for Nanophase Materials Sciences, Oak Ridge National Laboratory, P.O. Box 2008, Oak Ridge, TN 37831-6496, United States*

ARTICLE INFO

ABSTRACT

We demonstrate the use of copper underpotential deposition (UPD) for measurement of the electrochemically active surface area of a protein-modified gold electrode. The kinetics of adsorption and the subsequent structural rearrangement of β-casein, as a model protein, on the surface of a gold electrode have been followed over time. The protein-free surface area was determined by measuring the charge derived from UPD copper deposition on the non-blocked surface area at different stages of adsorption. The behaviour of β-casein adsorption as a function of surface roughness and the microstructure of the gold electrode, as well as the concentration of the protein solution, are studied using this method.

1. Introduction

Understanding and controlling protein adsorption and assembly on noble metal surfaces is important for the development of electrochemical biosensors, with applications ranging from virus protein and antibody detection, artificial olfactory sensing, early detection of cardiovascular disease and cancer signals to environmental risk assessment [1-5] .

A wide range of analytical techniques can be used to quantify the amount of adsorbed protein on a surface, including quartz-crystal microbalance, infrared spectroscopy, surface plasmon resonance, ellipsometry, optical waveguide lightmode spectroscopy, and atomic force microscopy [6-20]. However, these methods do not provide information about protein adsorption from the reactive metallic surface point of view, which is essential in electrochemical biosensor development. They are also poor in dealing with non-flat 3D structured surfaces, which are often selected to increase the surface area of the sensor.

Underpotential deposition (UPD) of a metal is an electrochemical process in which adsorbed metal atoms are deposited from a solution onto a foreign metal surface at an electrode potential which is more positive than the equilibrium potential of the metal deposition/dissolution in the same system given by the Nernst equation. The driving force of UPD is the adsorption energy of the metal atoms on the foreign metal surface. Thermodynamic and kinetic descriptions of this phenomenon can be found in several reviews [21-24]. Gold has been studied

both as a substrate and as a deposited metal [25-27]. Since the adsorption of metal atoms is very sensitive to the atomic arrangement and structure of the substrate metal, UPD can be used for characterization of the surfaces, especially in the case of noble metals, as demonstrated by a recent review [28] and references therein. Copper UPD on gold single crystals as well as polycrystalline electrodes has been investigated extensively and it is well established that anions have a considerable effect on the underpotential deposition [28-30].

The adatom probe method has already been used to investigate protein adsorption processes [31-33], but the parallel metal–protein complex formation [34] in solution might lead to complicated surface phenomena and the interesting features of metal–protein co-adsorption could interfere with the UPD process. As a mirror approach in a sensor-related functional application, UPD copper was used to fill an uncovered sensor surface to minimize unspecific protein adsorption [35].

Application of nanostructured electrode surfaces in sensor development offers new properties, from surface-area-related signal enhancement to tunable biomolecule functionality due to the size-matching adsorption sites of biomolecules on different nanoscale structures [7,36,37].

In this work we aim to give more insight into the precision application of the adatom probe method based on the underpotential deposition of copper to follow protein adsorption on nanostructured gold surfaces. Copper was deposited from a Cu^{2+}-ion-containing solution on an already partially protein-blocked surface, leading to the adsorption of

---

an amount of UPD copper that was solely proportional to the uncovered, electrochemically active clean gold surface. The method described is a convenient and explicit approach to determine surface coverage of a gold electrode by biomolecules and can be incorporated into the workflow of protein sensor development.

2. Materials and methods

2.1. Preparation and characterization of gold electrode surfaces with different electroactive surface areas

Round disk gold electrodes (Pine Research Instrumentations, USA) with diameter of 1.6 or 2 mm were used in the experiments. Electrochemical measurements were carried out in 3-compartment electrochemical cells, using a hydrogen electrode as the reference, and a large platinum sheet as the counter electrode. All electrode potentials quoted are on the RHE scale. The supporting electrolyte was 0.5 M H_2SO_4 prepared from concentrated p.a. sulfuric acid (Merck) and MilliQ water (18.2 MΩ.cm2). The solutions were deoxygenated with argon gas.

Galvanostatic gold deposition was used in order to increase the electroactive surface area (Au/Au) of the polished gold electrodes (Au). Gold was deposited from 2.5×10^{-3} M $HAuCl_4$ solution in 0.1 M H_2SO_4. Electrode surface characterization was performed by recording cyclic voltammograms on the different gold surfaces in deaerated 0.5 M H_2SO_4 solutions.

The electrochemically active real surface of the gold electrode was determined from the charge corresponding to the oxide-reduction peak on the cyclic voltammogram of the gold electrode at 1.8 V anodic potential limit, using the generally accepted assumption that 386 μC charge corresponds to 1 cm^2 active gold surface [38]. The roughness factor (RF) is used in the normal sense: RF = real surface area/geometric surface area.

In order to demonstrate the formation of a microstructure on the rough surfaces, SEM images of the gold layers electrodeposited on smooth gold electrodes were recorded using a ZEISS Merlin Field Emission Scanning Electron Microscope.

2.2. Protein adsorption and copper underpotential deposition measurements

The kinetics of protein adsorption were determined through measurement of the amount of copper deposited on a protein-free surface, and then on a protein-covered surface. In order to determine the maximum amount of UPD copper on a given surface, copper was deposited from 0.5 M H_2SO_4 solution containing 10^{-3} M Cu^{2+} at 400 mV for t = 2 min. The deposited copper was measured through its reoxidation by a linear potential sweep in the 400 mV to 750 mV range. This step also ensured that all deposited copper had been removed from the surface. After rigorous rinsing with MilliQ water, the electrodes were immersed in freshly prepared β-casein (Aldrich, >98%) solutions at concentrations of 0.05 mg/ml or 0.01 mg/ml in MilliQ water for different periods of time. After rinsing with MilliQ water the electrodes were subjected to copper underpotential deposition under the same conditions as before β-casein adsorption. The difference in the amount of deposited copper before and after protein adsorption was related to the area of the electrode surface covered by β-casein at a given time.

3. Results and discussion

3.1. Copper underpotential deposition for electrochemically active surface area characterization

Cyclic voltammograms of a gold electrode obtained in pure 0.5 M H_2SO_4 and in 0.5 M H_2SO_4 solutions containing 10^{-3} M Cu^{2+} can be seen in Fig. 1. Potentiostatic deposition at 400 mV was chosen for UPD copper deposition. At this voltage only the most strongly bonded adatoms are
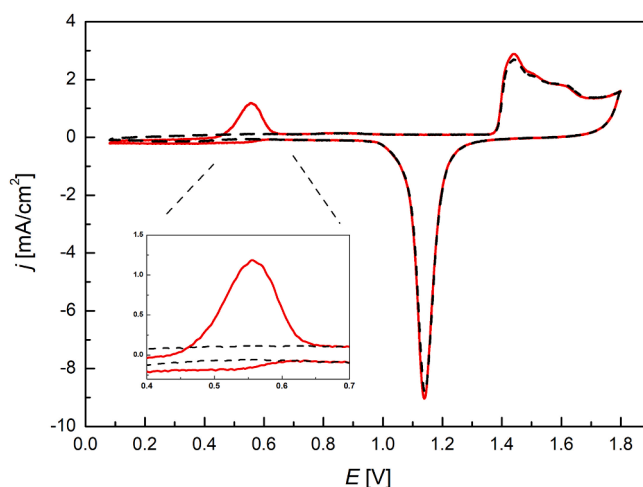

Fig. 1. Cyclic voltammogram of Au/Au electrode (R = 20) in 0.5 M H_2SO_4 (dashed black line) and in 0.5 M H_2SO_4 containing 10^{-3} M Cu^{2+} ions (solid red line), sweep rate 100 mV/s. (For interpretation of the references to colour in this figure legend, the reader is referred to the web version of this article.)

formed, ensuring that only adsorbed copper atoms were deposited on the gold surface, without any bulk copper deposition. A more detailed figure (Figure S1) can be found in the Supplementary Information – this gives information on the multiple energy states of copper electrodeposits, where in addition to the UPD copper deposited at 400 mV, bulk copper deposition at 150 mV is also demonstrated.

Fig. 2 shows the optimization of the UPD process, ie the potential sweeps obtained after holding the potential at 400 mV for different periods of time. In accordance with earlier results [19] the oxidation charge of the strongly bonded adsorbed copper reached a constant value after a relatively short time (about t = 1 min), and this charge was about one quarter of the charge of the oxide-reduction peak for the same electrode. Taking these results into consideration, t = 2 min was set as the standard deposition time for copper UPD.

3.2. Effect of roughness factor on protein adsorption kinetics

We first investigated the validity of the proposed method, namely
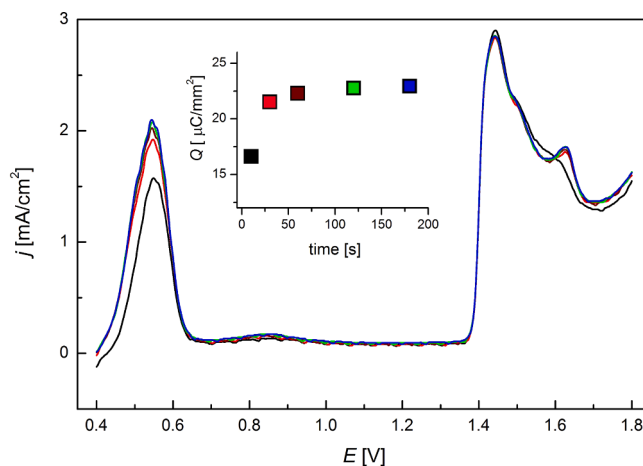

Fig. 2. Polarization curves of Au/Au electrode (R = 20) after holding the potential at 400 mV for 10 s (black), 30 s (red), 60 s (wine), 120 s (green) and 180 s (blue) in 0.5 M H_2SO_4 solution containing 10^{-3} M Cu^{2+} ions. Sweep rate 100 mV/s. Inset: Oxidation charge corresponding to the UPD Cu peak as a function of the time of deposition at 400 mV. (For interpretation of the references to colour in this figure legend, the reader is referred to the web version of this article.)

that during the copper deposition–dissolution processes, the previously adsorbed protein layer remains stable on the gold surface. Two types of tests were used to validate the method:

a) The copper deposition–dissolution steps were repeated on the same, partially casein-covered electrodes. It was found that the amount of UPD copper was the same, which indicated that the protein-covered part of the gold was unchanged.
b) The time of casein adsorption was divided into shorter intervals and the coverage was measured after each interval. It was found that the final coverage at a given electrode was independent of the number of intervals, depending only on the sum of the adsorption times. Two sequential 1-minute immersions in the β-casein solution resulted in the same β-casein coverage as a single 2-minute immersion.

The coverage vs. adsorption time correlation is sensitive to the roughness of the gold surface, as demonstrated by Fig. 3, Fig. S2 and Fig. 4. In Fig. 4 three Au/Au electrodes prepared by galvanostatic Au deposition with different surface roughness ($R = 14$, $R = 22$ and $R = 50$) are compared. All the deposition parameters were identical except for the time of gold deposition. The shapes of the voltammetric curves are practically the same (Fig. 4 insets); only the current range is different. The ratios of the electrochemically active surface areas were 1:1.6:3.5 calculated from the oxide-reduction peak and from the charges related to the oxidation of UPD Cu on the bare electrodes. SEM images revealing the formation of complex structures in the electrodeposited gold layers are shown in Fig. S3.

The β-casein adsorption experiments were performed using 1–15-minute time intervals, and copper UPD was conducted before and after protein adsorption. Copper stripping curves are depicted in Fig. 3 and Fig S2 and the measured currents were normalized to the geometric surface area of the electrode.

The relative decrease in the uncovered gold area measured as a function of casein adsorption time was obtained from the following equation:

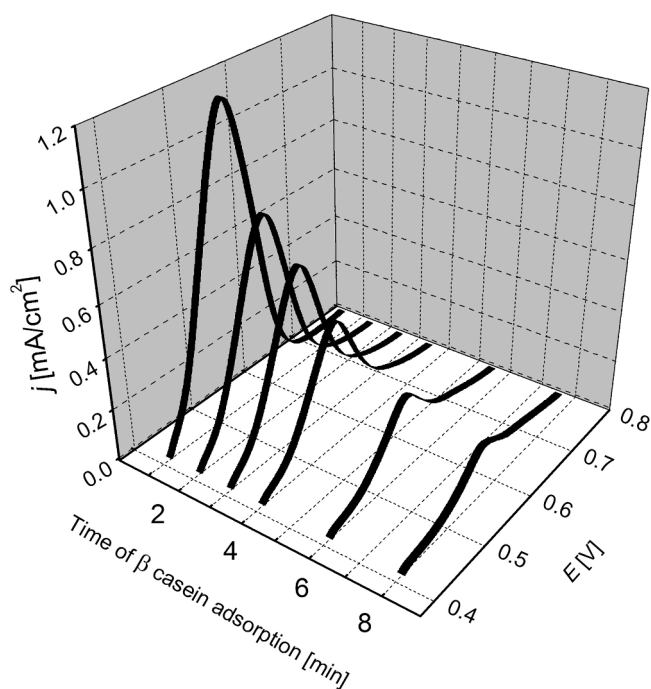$$(1 - \Theta)_{Au} = Q_{(Cu,ox,t)}/Q_{(Cu.ox,0)}$$

Fig. 3. Decrease in the stripping peak of UPD Cu on Au/Au ($R = 14$) electrode as a function of time of β-casein adsorption from a solution of 0.05 mg/ml β-casein in MilliQ water. Sweep rate: 100 mV/s.
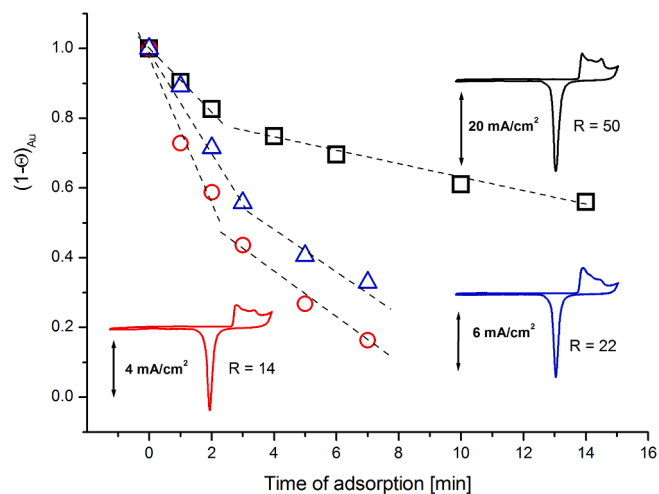

Fig. 4. Changes in β-casein-free surface of Au/Au ($R = 14$) (red circles), Au/Au ($R = 22$) (blue triangles) and Au/Au ($R = 50$) (black squares) electrodes as a function of the time of β-casein deposition from a solution of 0.05 mg/ml β-casein in MilliQ water. Insets: CVs of the electrodes before β-casein adsorption, sweep rate: 100 mV/s. (For interpretation of the references to colour in this figure legend, the reader is referred to the web version of this article.)

where Θ is the coverage of the gold surface by β-casein, $Q_{(Cu,ox,t)}$ is the oxidation charge of the UPD copper deposited after holding the gold electrode in casein solution for time interval t, and $Q_{(Cu,ox,0)}$ is the oxidation charge of the UPD copper deposited on the bare gold electrode. The time intervals for casein adsorption on a given electrode were accumulated within a series of measurements. Fig. 4 shows that the Cu UPD method makes it possible to precisely observe that the coverage values are higher for electrodes with lower surface roughness for all adsorption times.

3.3. Effect of β-casein concentration on protein adsorption kinetics

To study the effect of β-casein concentration on the adsorption kinetics, two nearly identical Au/Au electrodes ($R = 22$ and $R = 24$) were prepared, and the adsorption was followed in solutions containing β-casein at concentrations of 0.05 mg/ml or 0.01 mg/ml. The CVs of the clean gold surfaces are shown in the inset of Fig. 5. The adsorption curves clearly indicate the different behaviour exhibited in the different solutions, but also reveal an interesting phenomenon in the case of the more dilute β-casein solution, namely that after certain time (between 3 and 5 min adsorption time in Fig. 5), instead of increased coverage a slight decrease could be observed. This observation was reproducible and, at certain β-casein concentrations and gold surface roughness values, a temporary increase in the uncovered gold surface of as much as 5–10% could be detected. This phenomenon can be explained by the interference of two types of surface-related process kinetics: simple adsorption kinetics and the surface conformational kinetics of biomolecules. The results indicate that the Cu UPD method can detect the rearrangement of the already adsorbed β-casein molecules, resulting in layer densification.

3.4. Effect of gold microstructure on protein adsorption kinetics

It is important to understand that different gold microstructures, even with a similar roughness factor, may have a considerable effect on the protein adsorption process. Fig. 6 shows that the adsorption capacity of the gold surface and the β-casein adsorption rate may be different on differently prepared gold surfaces with the same surface roughness. The electrodes were prepared by depositing gold from the same solution but using different current densities and deposition times. The inset of Fig. 6 shows cyclic voltammograms of the freshly prepared electrodes,
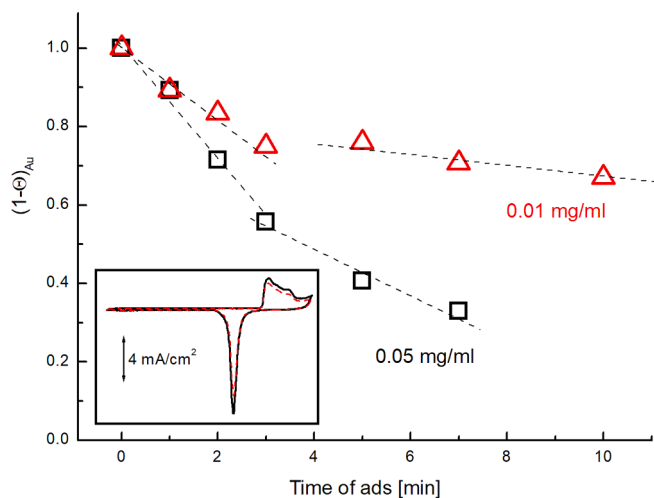
Fig. 5. Changes in β -casein-free surface of two similar Au/Au electrodes ($R = 24$ and $R = 22$) as a function of β -casein deposition time in β -casein solutions of concentration 0.05 mg/ml (black squares) and 0.01 mg/ml (red triangles). Inset: CVs of the Au/Au electrodes measured in 0.5 M H_2SO_4 solution before β -casein adsorption, sweep rate: 100 mV/s. (For interpretation of the references to colour in this figure legend, the reader is referred to the web version of this article.)
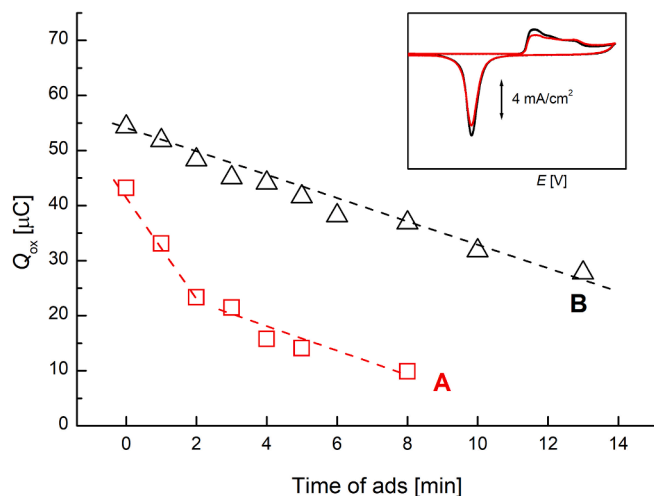

Fig. 6. Change in the oxidation charge of UPD Cu with the time of β -casein adsorption from a solution of 0.05 mg/ml β -casein in MilliQ water on two Au/Au electrodes of similar surface roughness ($R = 14$ and $R = 19$) prepared using different gold deposition parameters. Inset: CVs measured on freshly prepared Au/Au electrodes in 0.5 M H_2SO_4 solution, sweep rate: 100 mV/s.

indicating that the gold surfaces have nearly identical surface roughness values ($R = 14$ and $R = 19$).

Fig. 6 shows the raw data of the charge measured during dissolution of the UPD copper (i.e. without normalization to adsorption on a β -casein-free clean gold surface). The gold electrode surfaces show different adsorption capacities: for example, during the first minute of immersion the decrease in charge corresponding to the oxidation of UPD copper was 10 μ C on electrode A, but only 2.5 μ C on electrode B. The 10 μC decrease in the UPD copper stripping peak is equivalent to a Au surface loss of 10 mm^2, while in the case of electrode B only 2.5 mm^2 of the gold surface had been covered during the first minute of casein adsorption. For comparison, the electrodes presented in Fig. 4, which differ solely in deposition time, which produced a clear difference in roughness ($R = 14$ and $R = 50$), lost similar areas of 10 mm^2 and 12 mm^2, respectively, from their uncovered surface area during the first

minute of adsorption. These results support our claim that the Cu UPD method is sensitive enough to reveal microstructural features on electrodes that can be significant from the point of view of biomolecule adsorption.

4. Conclusions

Copper underpotential deposition was used as an indirect method to study protein adsorption kinetics on structured gold electrodes. This method of measuring the protein-free gold surface though Cu UPD oxidation was used to study the influence of the electrode roughness factor and morphological variations, as well as the solution phase protein concentration. This method highlights details of the adsorption process from the adsorbent side and gives important information about the process usually described from data based on the amount of adsorbed material. The described methodology would be particularly useful for electrochemical biosensor design and in the measurement of precise surface coverage.

CRediT authorship contribution statement

István Bakos: Conceptualization, Methodology, Investigation, Visualization, Writing - original draft, Writing - review & editing. **Ádám Vass:** Investigation, Validation, Writing - review & editing. **Eric S. Muckley:** Investigation, Validation, Writing - review & editing. **Ilia N. Ivanov:** Conceptualization, Visualization, Project administration, Funding acquisition, Writing - review & editing. **Zsófia Keresztes:** Visualization, Project administration, Funding acquisition, Writing - original draft, Writing - review & editing.

Declaration of Competing Interest

The authors declare that they have no known competing financial interests or personal relationships that could have appeared to influence the work reported in this paper.

Acknowledgement

Appendix A. Supplementary data

Supplementary data to this article can be found online at https://doi.org/10.1016/j.elecom.2021.106961.

Reference

[1] M.R. de Eguilaz, L.R. Cumba, R.J. Forster, Electrochem. Commun. 116 (2020), 106762, https://doi.org/10.1016/j.elecom.2020.106762.
[2] A.J.M. Barbosa, A.R. Oliveira, A.C.A. Roque, Trends Biotechnol. 36 (2018) 1244–1258, https://doi.org/10.1016/j.tibtech.2018.07.004.
[3] K.S. Song, S.B. Nimse, M.D. Sonawane, S.D. Warkad, T. Kim, Sensors (Switzerland) 17 (2017) 2116, https://doi.org/10.3390/s17092116.
[4] J.M. Lim, M.Y. Ryu, J.W. Yun, T.J. Park, J.P. Park, Biosens. Bioelectron. 98 (2017) 330–337, https://doi.org/10.1016/j.bios.2017.07.013.
[5] S. Ray, S. Panjikar, R. Anand, ACS Sensors 3 (2018) 1632–1638, https://doi.org/10.1021/acssensors.8b00190.
[6] S. Boujday, A. Bantegnie, E. Briand, P.G. Marnet, M. Salmain, C.M. Pradier, J. Phys. Chem. B 112 (2008) 6708–6715, https://doi.org/10.1021/jp711916g.
[7] Z. Adamczyk, A. Pomorska, M. Nattich-Rak, M. Wytrwal-Sarna, A. Bernasik, J. Colloid Interface Sci. 530 (2018) 631–641, https://doi.org/10.1016/j.jcis.2018.06.063.
[8] M. Dargahi, S. Omanovic, Colloids Surfaces B Biointerfaces 116 (2014) 383–388, https://doi.org/10.1016/j.colsurfb.2013.12.028.

[9] H. Arwin, Thin Solid Films 377–378 (2000) 48–56, https://doi.org/10.1016/S0040-6090(00)01385-7.

[10] M.A. McArthur, T.M. Byrne, R.J. Sanderson, G.P. Rockwell, L.B. Lohstreter, Z. Bai, M.J. Filiaggi, J.R. Dahn, Colloids Surfaces B Biointerfaces 81 (2010) 58–66, https://doi.org/10.1016/j.colsurfb.2010.06.024.

[11] E. Servoli, D. Maniglio, M.R. Aguilar, A. Motta, J. San Roman, L.A. Belfiore, C. Migliaresi, Macromol. Biosci. 8 (2008) 1126–1134, https://doi.org/10.1002/mabi.200800110.

[12] P. Schön, M. Görlich, M.J.J. Coenen, H.A. Heus, S. Spelled, Langmuir 23 (2007) 9921–9923, https://doi.org/10.1021/la700236z.

[13] E. Migliorini, M. Weidenhaupt, C. Picart, Biointerphases 13 (2018) 06D303, https://doi.org/10.1116/1.5045122.

[14] M. Tatarko, E.S. Muckley, V. Subjakova, M. Goswami, B.G. Sumpter, T. Hianik, I. N. Ivanov, Sensors and Actuators B: Chemical 272 (2018) 282–288, https://doi.org/10.1016/j.snb.2018.05.100.

[15] E.S. Muckley, L. Collins, B.R. Srijanto, I.N. Ivanov, Adv. Funct. Mater. 30 (2020) 1908010, https://doi.org/10.1002/adfm.201908010.

[16] E.S. Muckley, C.B. Jacobs, K. Vidal, J.P. Mahalik, R. Kumar, B.G. Sumpter, I. N. Ivanov, A.C.S. Appl, Mater. Interfaces 9 (2017) 15880–15886, https://doi.org/10.1021/acsami.7b03128.

[17] Z. Keresztes, P.G. Rouxhet, C. Remacle, C. Dupont-Gillain, J. Biomed. Mater. Res. 76A (2006) 223–233, https://doi.org/10.1002/jbm.a.3047.

[18] B. Kovacs, A. Saftics, A. Biro, S. Kurunczi, B. Szalontai, B. Kakasi, F. Vonderviszt, A. Der, R. Horvath, J. Phys. Chem. C 122 (2018) 21375–21386, https://doi.org/10.1021/acs.jpcc.8b05026.

[19] E. Agocs, P. Kozma, J. Nador, A. Hamori, M. Janosov, B. Kalas, S. Kurunczi, B. Fodor, E. Ehrentreich-Förster, M. Fried, R. Horvath, P. Petrik, Appl. Surf. Sci.Part B 421 (2017) 289–294, https://doi.org/10.1016/j.apsusc.2016.07.166.

[20] B. Jin, W.J. Bao, Z.Q. Wu, X.H. Xia, Langmuir 28 (2012) 9460–9465, https://doi.org/10.1021/la300819u.

[21] D.M. Kolb, in: H. Gerischer, C.W. Tobias (Eds.), Adv. Electrochem. Electrochem. Eng., vol. 11, John Wiley, New York, 1978, p. 125.

[22] R.R. Adzic, in: H. Gerischer, C.W. Tobias (Eds.), Adv. Electrochem. Electrochem. Eng., vol. 13, John Wiley, New York, 1984, p. 159.

[23] G. Kokkinidis, J. Electroanal. Chem. 201 (1986) 217–236, https://doi.org/10.1016/0022-0728(86)80051-1.

[24] S. Szabó, Int. Rev. Phys. Chem. 10 (1991) 207–248, https://doi.org/10.1080/01442359109353258.

[25] I. Bakos, S. Szabó, T. Pajkossy, J. Solid State Electrochem. 15 (2011) 2453–2459, https://doi.org/10.1007/s10008-011-1444-2.

[26] I. Bakos, S. Szabó, J. Electroanal. Chem. 369 (1994) 223–226, https://doi.org/10.1016/0022-0728(94)87102-7.

[27] I. Bakos, S. Szabó, J. Electroanal. Chem. 344 (1993) 303–311, https://doi.org/10.1016/0022-0728(93)80062-M.

[28] N. Mayet, K. Servat, K.B. Kokoh, T.W. Napporn, Surfaces 2 (2019) 257–276, https://doi.org/10.3390/surfaces2020020.

[29] M.C. Santos, L.H. Mascaro, S.A.S. Machado, Electrochim. Acta 13 (1998) 2263–2272, https://doi.org/10.1016/S0013-4686(97)10171-2.

[30] A.J. Motheo, E.R. Gonzalez, A. Rakotondrainibe, J.M. Léger, B. Beden, C. Lamy, J. Braz. Chem. Soc. 7 (1996) 1–6, https://doi.org/10.5935/0103-5053.19960001.

[31] B. Bozzini, S.A. Campbell, L. D'Urzo, Trans. Inst. Met. Finish. 85 (2007) 123–134, https://doi.org/10.1179/174591907X192276.

[32] M. Hepel, M. Stobiecka, Bioelectrochemistry 70 (2007) 155–164, https://doi.org/10.1016/j.bioelechem.2006.03.032.

[33] S. Murray, L. Cros, Colloids and Surfaces B: Biointerfaces 10 (1998) 227–241, https://doi.org/10.1016/S0927-7765(97)00066-0.

[34] S. Mannino, M. Bianco, F. Bonomi, Food Chemistry 24 (1987) 159–165, https://doi.org/10.1016/0308-8146(87)90047-1.

[35] X. Liu, X. Wang, J. Zhang, H. Feng, X. Liu, D.K.Y. Wong, Biosens. Bioelectron. 35 (2012) 56–62, https://doi.org/10.1016/j.bios.2012.02.002.

[36] K.J. Stine, Appl. Sci. 9 (2019) 797, https://doi.org/10.3390/app9040797.

[37] B.M. Manzi, M. Werner, E.P. Ivanova, R.J. Crawford, V.A. Baulin, Sci. Rep. 9 (2019) 4694, https://doi.org/10.1038/s41598-019-40920-z.

[38] R.R. Woods, in: A.J. Bard (Ed.), Electroanal. Chem., vol. 9, Marcel Dekker Inc., New York and Basel, 1976, p. 2.